

Short Communication

## Rhombohedral-structured $\text{LiVO}_2$ Prepared by a Novel Two-Step Method and Its Electrochemical Properties

Xiaohui Li, Zhi Su\*, Huanling Tian, Yanhui Zhang

College of Chemistry and Chemical Engineering, Xinjiang Normal University, Urumqi, 830054, Xinjiang, China

\*E-mail: [suzhixj@sina.com](mailto:suzhixj@sina.com)

Received: 23 October 2016 / Accepted: 4 December 2016 / Published: 12 December 2016

---

Layered  $\text{LiVO}_2$  was prepared as a cathode material for lithium ion batteries by a novel two-step reduction method. The structure and morphology of the material were characterized by X-ray diffraction, X-ray photoelectron spectroscopy, and transmission electron microscopy. The specific capacity of the material reached  $201.7 \text{ mAh g}^{-1}$  when charged and discharged at a rate of 0.2 C in the voltage range of 1.0–4.5 V. The retention ratio of discharge capacity was 65% after 30 cycles. The charge-transfer resistance calculated by fitting the experimental electrochemical impedance data to the equivalent circuit model was  $81.65 \Omega$ . From this, the lithium ion diffusion coefficient was calculated to be  $2.72 \times 10^{-11} \text{ cm s}^{-1}$ , indicating that this material exhibits excellent ionic and electronic conductivity.

---

**Keywords:**  $\text{LiVO}_2$ ; two-step method ; cathode materials; electrochemical performance

### 1. INTRODUCTION

Layered rock-salt type  $\text{LiMO}_2$  oxides (where M = Co, Ni, Mn, etc.) have attracted much attention as high energy density cathode materials for lithium rechargeable batteries [1–3]. Among the various  $\text{LiMO}_2$  oxides,  $\text{LiCoO}_2$  has become one of the primary cathode materials used in commercial lithium-ion batteries. However, it has a number of drawbacks. Cobalt resources are scarce, expensive, and toxic and the cycle performance of  $\text{LiCoO}_2$  is poor. Another candidate is  $\text{LiNiO}_2$  [4], which has advantages such as having low self-discharge and being non-polluting. However, it also has many shortcomings such as being difficult to synthesize, having poor structural order, poor cycle performance, and safety issues during the electrochemical reactions. On the other hand, owing to its low cost,  $\text{LiMnO}_2$  [5] is environmentally acceptable and manganese resources are easily available. However,  $\text{LiMnO}_2$  undergoes irreversible phase change to  $\text{Li}_2\text{Mn}_2\text{O}_4$  with the quartet spinel structure

and  $\text{Li}_x\text{Mn}_2\text{O}_4$  with the cubic spinel structure during the lithium ion insertion and extraction processes during cycling, causing capacity degradation.

$\text{LiVO}_2$  crystallizes into a rhombohedral structure, with the  $R\bar{3}m$  space group and with hexagonal lattice constants  $a=2.83 \text{ \AA}$  and  $c=14.87 \text{ \AA}$  [6]. The  $\text{LiVO}_2$  structure consists of successive layers of vanadium, oxygen, and lithium ions. The vanadium and lithium ions occupy the octahedral sites in the cubic close packed lattice of oxygen ions and the  $\text{LiVO}_2$  exhibits layered quasi-2D characteristics [7-8].

There have been a limited number of literature reports on the electrochemical properties of layered  $\text{LiVO}_2$ . The current method of synthesis of  $\text{LiVO}_2$  is based on conventional solid-state reaction and hydrothermal synthesis. However, the specific capacity of layered  $\text{LiVO}_2$  synthesized by this method has been reported to be only 50-100  $\text{mAh g}^{-1}$ , owing to the irreversible structural change that occurs upon delithiation [9-10]. Although in several studies, many researchers tried to change synthesis method or combined with other material in order to promotion electrochemical capability of  $\text{LiVO}_2$ , most of the reports do not improved greatly electrochemical capability for this material. In the present article, we report the preparation of a layered  $\text{LiVO}_2$  compound as a cathode material for lithium-ion batteries by a novel two-step reduction method with sucrose as the reducing agent. Through a series of tests, the electrochemical properties of the  $\text{LiVO}_2$  electrode material have been characterized.

## 2. EXPERIMENTAL

### 2.1 Preparation of $\text{LiVO}_2$

$\text{LiVO}_2$  was synthesised by a two-step reduction.  $\text{LiAc}$ , sucrose and  $\text{V}_2\text{O}_5$  were used as the starting materials. First, 0.91 grams of  $\text{V}_2\text{O}_5$  was dissolved in 20 mL deionized water with magnetic stirring. Next, an appropriate amount of  $\text{H}_2\text{O}_2$  (about 20 mL) was added slowly to the previous seriflux until it became an orange apparent solution. After that, stoichiometric ratio of  $\text{LiAc}$  and sucrose (dissolved respectively in 50 mL deionized water) was added to the solution slowly in the same way over 2 h at room temperature. The mixture was then removed to a vacuum oven and dried for 24 h at 80 °C, which led to the formation of a brownish black solid. This solid was ground into a powder, which was placed in a small crucible and calcined at 400 °C for 4 h, followed by heating at 750 °C for 12 h under a flowing argon atmosphere.

### 2.2 Characterization

The crystal structures of the samples were investigated by X-ray diffraction (XRD, Bruker D2, Germany) with  $\text{Cu K}\alpha$  radiation. The XRD data were collected using the step mode over an angular range of 10–70° with a step size of 0.02° at voltage and current values of 30 kV and 10 mA, respectively. The morphology of the sample was analyzed using transmission electron microscopy

(TEM, Philips CM10) at an accelerating voltage of 200 kV. The electronic state of each element was characterized by X-ray photoelectron spectroscopy (XPS, ESCALAB 250Xi).

### 2.3 Electrochemical properties

The charge and discharge characteristics of the  $\text{LiVO}_2$  electrode were examined using a battery testing system (LAND CT-2001A, Wuhan, China) at a charge/discharge rate of 0.2 C in the voltage range of 1.0–4.5 V at room temperature. The cathode consisted of the active material, acetylene black, and polytetrafluoroethylene (PTFE) in a weight ratio of 80:15:5. This mixture was added to a certain amount of deionized water to form a slurry after sufficient stirring. The slurry was coated on an aluminum current collector, and then dried in a vacuum oven at 110°C for 12 h. This was used as the cathode material. Finally, the electrochemical cells were assembled in an argon-filled glove box using this cathode with lithium slices as the anode and a solution of 1 M  $\text{LiPF}_6$  in a mixture of ethylene carbonate (EC)/dimethyl carbonate (DMC) (1:1 v/v) as the electrolyte. The charge-discharge profiles and cycle life of the cells were measured using a battery testing instrument (LAND, CT-2001A) at a rate of 0.2 C in the voltage range of 1.0–4.5 V. The electrochemical properties of the cell were measured using an electrochemical workstation (LK2005A, Tianjin, China), Cyclic voltammetry (CV) measurements were conducted in the voltage range of 1.0–4.5 V at a scan rate of 0.1  $\text{mV s}^{-1}$ . Electrochemical impedance spectroscopy (EIS) measurements were performed over the frequency range of 0.01 Hz to 0.1 MHz after the electrochemical tests.

## 3. RESULTS AND DISCUSSION

The XRD patterns of the samples synthesized by the two-step reduction method are shown in Fig. 1(a). From the figure, it is evident that all the diffraction peaks of  $\text{LiVO}_2$  exactly match the standard card of  $\text{LiVO}_2$  with the  $R\bar{3}m$  space group symmetry [11-12]. There are no foreign peaks detected and all the peaks are sharp and intense, implying that the prepared sample consists of a single phase with a high degree of crystallinity.

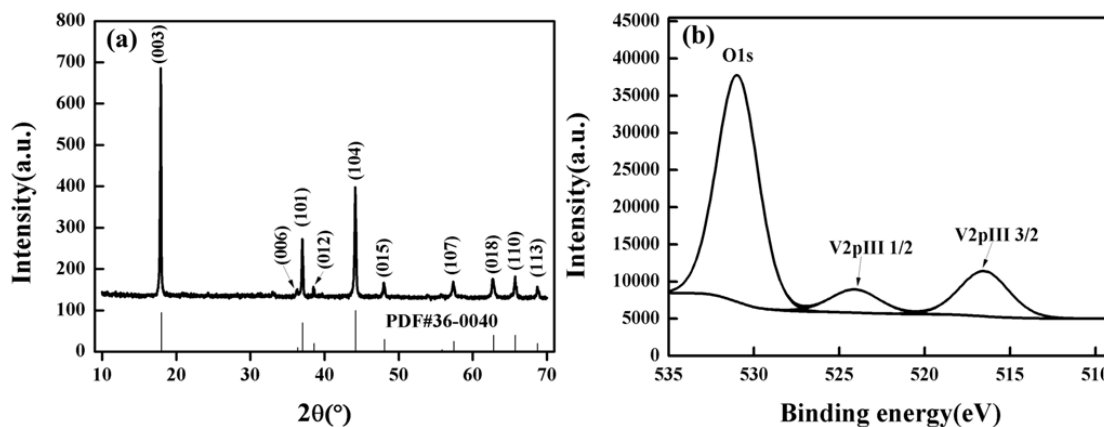


**Figure 1.** (a) X-ray diffraction profiles of  $\text{LiVO}_2$  composites at 750°C; (b) XPS survey spectrum of the as-prepared sample

The XPS survey spectrum of  $\text{LiVO}_2$  is shown in Fig. 1(b). The oxidation state of vanadium in the initial  $\text{V}_2\text{O}_5$  material is +5. The oxidation state of vanadium in  $\text{LiVO}_2$  was determined from the V 2p spectrum in the binding energy range of 510–535 eV. The V 2p spectrum mainly consists of V  $2p_{3/2}$  and V  $2p_{1/2}$  peaks at binding energies of 516.97 eV and 524.06 eV, respectively [13]. The peak position is consistent with  $\text{V}^{3+}$ . The results show that the valence state of vanadium ions in  $\text{LiVO}_2$  is +3.

TEM images of the samples are shown in Fig. 2. From the images, it is evident that the particle size of the synthesized material ranges from 20–50 nm. The particles are also non-uniform in size and agglomerate at high calcination temperatures. The lattice spacing of 0.203 nm corresponds to the interplanar distance of the (104) plane in the layered rock-salt structure of the  $R\bar{3}m$  phase. The light gray region in the figure corresponds to the carbon layer, which is attached to the surface of the material, forming a carbon film with a thickness of 0.425 nm.

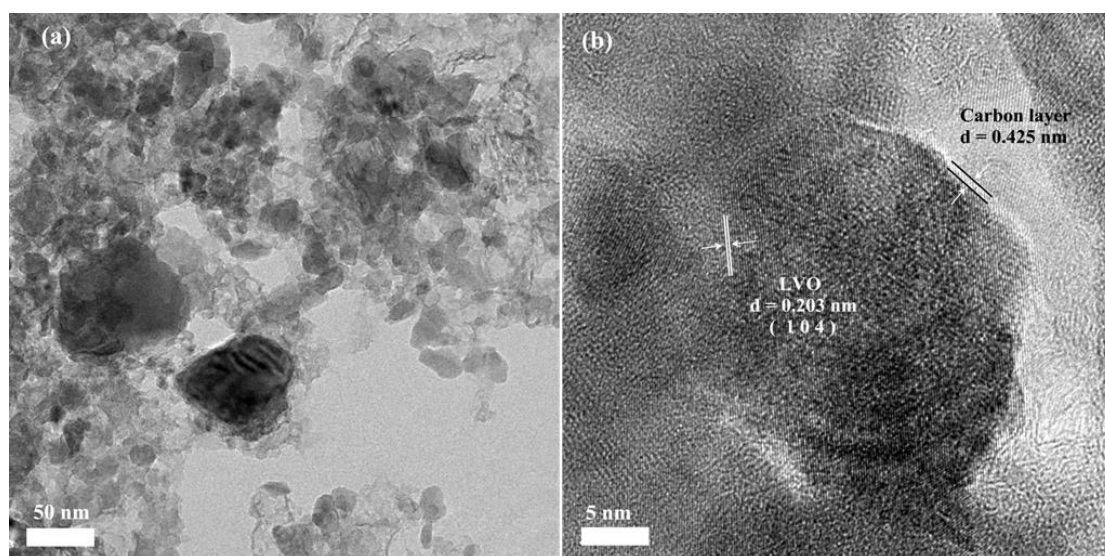


**Figure 2.** TEM images of  $\text{LiVO}_2$  at different magnifications: (a)  $4 \times 10^{-4}$  scale and (b)  $4 \times 10^{-5}$  scale.

The charge-discharge curves of  $\text{LiVO}_2$  measured at a rate of 0.2 C between 1.0 to 4.5 V are shown in Fig. 3(a). The first discharge capacity of the material is  $201.7 \text{ mAh g}^{-1}$ . After 30 cycles, a discharge capacity of  $130.8 \text{ mAh g}^{-1}$  is still retained, which corresponds to 65% retention of the initial capacity. Fig. 3(b) presents the cycling performance of the  $\text{LiVO}_2$  composites measured at a charge/discharge rate of 0.2 C between 1.0 and 4.5 V. The results indicate that charge and discharge capacity of this system decreased drastically after the first cycle because  $\text{LiVO}_2$  quickly loses its electrode activity upon cycling, similar to  $\text{LiFeO}_2$ . This may be caused by the migration of vanadium ions from the transition metal layers to the lithium layer during the initial charging process [11]. The structural change prevents lithium ions from being back to their original sites, resulting in poor reversibility. But the reversible capacity of sample about  $130 \text{ mAh g}^{-1}$  incline to stabilized and almost no decay after 30 cycles, illustrating the  $\text{LiVO}_2$  which synthesized by a two-step reduction method has good reversibility and stability. The good electrochemical performance maybe due to introduced a traces of carbon and obtained finer particles via sol-gel method at first step, which increased the tap

density and reduced  $\text{Li}^+$  diffusion pathway lead to good cycling performance and electrochemical capability.

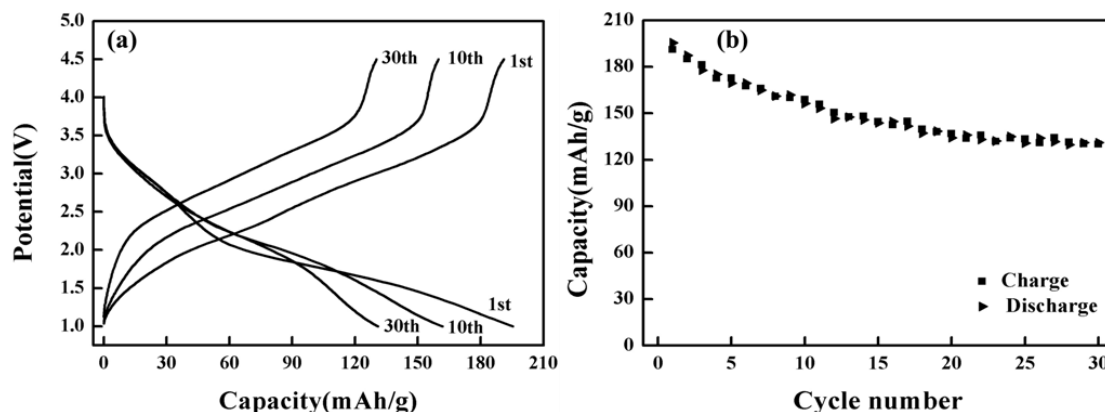


**Figure 3.** (a) The charge-discharge curves and (b) cycling performance of the  $\text{LiVO}_2$

In order to understand the reaction that occurs during the electrochemical process, cyclic voltammetry was conducted between 1.0 and 4.5 V at a scan rate of  $0.1 \text{ mV s}^{-1}$ . As observed in Fig. 4(a), there is an obvious oxidation peak at 3.96 V and a small reduction peak around 2.33 V. The large potential difference between the oxidation and reduction peaks indicates poor reversibility. With increase in the cycle number, the peaks become more sharp, corresponding to the charge-discharge platforms. This implies that the sample has poor reversibility as well as poor stability, which impact the cycle performance. EIS data for the  $\text{LiVO}_2$  composite are shown in Fig. 4(b). A semicircle in the high frequency range and a straight line at an angle to the real axis in the low frequency range are observed in the Nyquist plot.

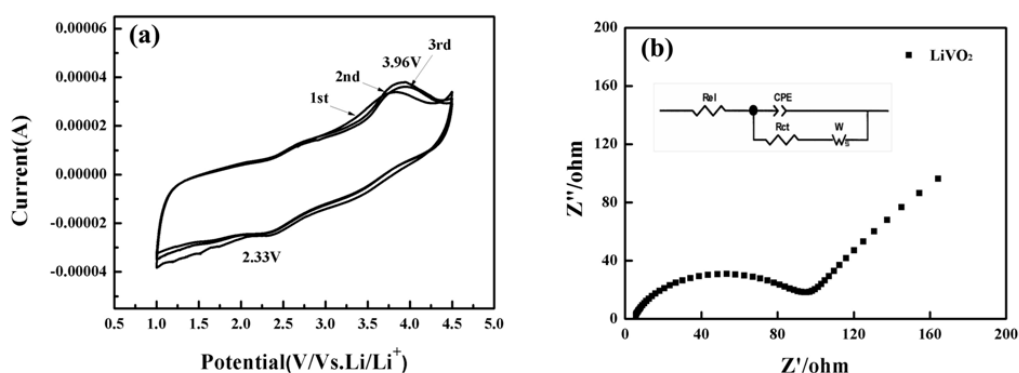


**Figure 4.** (a) The CV curve and (b) the EIS of the  $\text{LiVO}_2$  sample.

The semicircle in the high frequency range is mainly related to the electrochemical reaction at the electrolyte/cathode interface and includes contributions from the particle-to-particle contact resistance, charge transfer resistance, and lithium ion insertion and extraction. On the other hand, the

inclined line in the low frequency region represents the Warburg resistance, which is related to the diffusion of lithium ions into the electrode material. The value of charge-transfer resistance obtained by fitting the experimental data to the simulated equivalent circuit model is 81.65  $\Omega$ . From this value, the lithium ion diffusion coefficient was calculated as  $2.72 \times 10^{-11}$  cm<sup>2</sup> s<sup>-1</sup>, which indicates that this material exhibits excellent ionic and electronic conductivity.

#### 4. CONCLUSION

Layered LiVO<sub>2</sub> was successfully synthesized by a novel two-step reduction method using sucrose as the reducing agent. The XRD patterns indicate that LiVO<sub>2</sub> crystallizes with a rhombohedral structure and belongs to the  $R\bar{3}m$  space group. The specific capacity of the material measured at 0.2 C is 201.7 mAh g<sup>-1</sup> in the voltage range of 1.0–4.5 V, the reversible capacity of the sample also can reach 130.8 mAh g<sup>-1</sup> after 30 cycles, 65% of the initial discharge capacity is retained. After 20 cycles, the reversible capacity of sample almost no decay demonstrated this material has good cycling performance. At the same time exhibits excellent ionic and electronic conductivities.

#### ACKNOWLEDGMENTS

The study was supported by the National Natural Science Foundation of China (No. 21661030)

#### References

1. L. Wu, Y. Zhang, Y. G. Jung, J. Zhang, *J. Power Sources.*, 299 (2015) 57.
2. C. C. Chang, J. Y. Kim, P. N. Kumta, *J. Electrochem. Soc.*, 149 (2001) A1114.
3. J. Barker, M. Y. Saidi, J. L. Swoyer, *Solid state ionics.*, 158 (2003) 261.
4. S. Muto, K. Tatsumi, Y. Kojima, H. Oka, H. Kondo, K. Horibuchi, Y. Ukyo, *J. Power Sources.*, 205 (2012) 449.
5. S. Chen, F. Cao, F. Liu, Q. Xiang, X. Feng, L. Liu, G. Qiu, *RSC Advances.*, 4 (2014) 13693.
6. J. Ahn, H. O. Si, J. H. Kim, B. W. Cho, S. H. Kim, *J. Electroceram.*, 32 (2014) 390.
7. W. Tian, M. F. Chisholm, P. G. Khalifah, R. Jin, B. C. Sales, S. E. Nagler, D. Mandrus, *Mater. Res. Bull.*, 39 (2004) 1319.
8. I. Tsuyumoto, Y. Nakakura, S. Yamaki, *J. Am. Ceram. Soc.*, 97 (2014) 3374.
9. K. Ozawa, L. Wang, H. Fujii, M. Eguchi, M. Hase, H. Yamaguchi, *J. Electrochem Soc.*, 153 (2006) A117.
10. J. H. Song, H. J. Park, K. J. Kim, Y. N. Jo, J. S. Kim, Y. U. Jeong, Y. U. Kim, *J. Power Sources.*, 195 (2010) 6157.
11. N. Yabuuchi, K. Kubota, M. Dahbi, S. Komaba, *Chem. Rev.*, 114 (2014) 11636.
12. G. J. Wang, H. P. Zhang, L. J. Fu, B. Wang, Y. P. Wu, *Electrochem. Commun.*, 9 (2007) 1873
13. S. Loquai, B. Baloukas, O. Zabeida, J. E. Klemberg-Sapieha, L. Martinu, *Sol. Energy Mater. Sol. Cells.*, 155 (2016) 60.
14. J. S. Huang, L. Yang, K. Y. Liu, *Mater. Chem. Phys.*, 128 (2011) 470.
15. Y. Si, Z. Su, Y. Wang, T. Ma, J. Ding, *New J. Chem.*, 39 (2015) 8971.